

PACS numbers: 68.37.Hk, 78.30.Jw, 78.67.Bf, 81.07.Nb, 81.16.Be, 82.35.-x, 82.80.Ej

Synthesis and Characterization of Polypyrrole by Ammonium Persulfate as Oxidizing Agent and Study of Its Nanoparticles

Ahmad Al-Hamdan^{1,2}, Ola Amer³, Ahmad Al-Falah^{2,4},
Ibrahim Al-Ghoraibi^{3,4}, Fawaz Al-Deri², and Mirna Jabbour⁵

¹*Department of Chemistry,
Al-furat University,
Deir ez-Zor, Syria*

²*Department of Chemistry,
Damascus University,
Damascus, Syria*

³*Department of Physics,
Damascus University,
Damascus, Syria*

⁴*Faculty of Pharmacy,
Arab International University,
Ghabaghib, Daraa Governorate, Syria*

⁵*Faculty of Pharmacy,
Damascus University,
Damascus, Syria*

In this work, pyrrole is polymerized by ammonium persulfate as oxidizing agent in methanol 40%. Pyrrole polymer is characterized by FTIR, XPS and EDX to determine the polymer structure. Morphology of resulting polymer is studied by SEM. Polymer structure consists of spherical particles with sizes of about 38 nm assembled together to form huge clusters. Pyrrole polymer has semi-crystalline structure; its particles consist of crystalline core with size of 15.1 nm, surrounded by an amorphous shell fraction. Particles' size by XRD data is of 35.59 nm. This size may be more accurate than SEM size as XRD sample includes larger number of particles than SEM sample.

У цій роботі пірол полімеризується персульфатом амонію як окиснювачем у метанолі 40%. Піролів полімер характеризується інфрачервоною спектроскопією на основі перетвору Фур'є, рентгенівською фотоемісійною спектроскопією й енергорозсіювальною рентгенівською аналізою для визначення полімерної структури. Морфологія одержаного полімеру вивчається сканувальною електронною мікроскопією. Структура полімеру складається зі сферичних частинок розмірами близько 38 нм,

зібраних разом для утворення величезних скупчень. Полімерний пірол має напівкристалічну структуру; його частинки складаються з кристалічного ядра розміром 15,1 нм, оточеного оболонкою аморфної фракції. Розмір частинок за даними рентгенівської дифракції становить 35,59 нм. Цей розмір може бути більш точним, аніж розмір за даними сканувальної електронної мікроскопії, оскільки зразок для рентгенівської дифракції включає більшу кількість частинок, ніж зразок для сканувальної електронної мікроскопії.

Key words: polymerization, pyrrole polymer, nanoparticles, semi-crystalline structure, XRD.

Ключові слова: полімеризація, піролів полімер, наночастинки, напівкристалічна структура, рентгенівська дифракція.

(Received 7 December, 2021; in revised form, 19 January, 2022)

1. INTRODUCTION

Polymers are usually used as insulators. Nevertheless, in fact, not all polymers are insulators. They can be conductive just like metals [1]. The first conducting polymer (polysulphur nitride) was discovered in 1975 [2], later on poly(acetylene) was discovered [3]. In recent years, conducting polymers have been synthesized from aromatic rings [4] such as benzene [5], pyridine [6], pyrrole, furan and thiophene [7].

They have been extensively studied because of their chemical stability [3] and wide applications [4]. Polypyrrole (PPy) is one of the most important [3] and widely studied conducting polymers [8] due to its high electric conductivity. Polypyrrole has some advantages over the other conducting polymers, such as easier synthesis in water solution [9], good electrochemical properties, thermal stability [10], and low-cost processing [1]. However, compared to PANI, cost of pyrrole monomers is greater than aniline, which makes it less attractive for some potential applications [10]. Chemical stability of oxidized PPy is very good at room temperature. PPy degradation happens only when the temperature is more than 150°C [11]. Electrical conductivity of PPy ranges from 10 to 1000 S/cm [3, 12].

Pyrrole can be polymerized by chemical and electrochemical polymerization. Electrochemical polymerization of PPy can be performed either in aqueous media or non-aqueous media such as acetonitrile [12], propylene carbonate [14, 15], and dichloromethane [11]. Corrosion-resistant materials such as Pt, Au, Pd, Rh, Ir, etc. [16, 17] are used as the working electrodes [3]. Polypyrrole had many applications, including batteries, electrochemical sensors, biosensors [18], drug delivery systems, conductive textiles, conducting

fabrics, and mechanical actuators [19]. In a typical chemical oxidative polymerization of PPy, many oxidants, such as ferric perchlorate, ferric chloride and ammonium peroxydisulfate, have been used [20]. Electrochemical synthesis method for polypyrrole may be preferred [3] because it is eco-friendly and does not contain environmentally toxic solvents, and its relatively easy working [3]. In this work, we have used an easy method for preparing polypyrrole by ammonium persulfate as an oxidizing agent in methanol 40%. The polypyrrole was characterized by FTIR, XPS, and EDX. Its particle sizes are characterized by means of the SEM and XRD techniques.

2. EXPERIMENTAL

2.1. Materials and Measurements

Pyrrole 98% sigma Aldrich, methanol 99% sigma Aldrich, ammonium persulfate sigma Aldrich, polypyrrole was characterized with FTIR (JASCO FT/IR model M4100) spectrophotometer between 4000 and 400 cm^{-1} . Surface morphologies were examined with SEM, EDX and XPS (TESCAN model MIRA3). X-ray diffraction is made by Philips model: PW1370, Cu (0.154056 nm) step size 0.05 deg.

2.2. Synthesis

Pyrrole solution (1 gr, 15 mmole in 10 ml of methanol 40%) and ammonium persulfate solution (7 gr, 30 mmole dissolved in 25 ml of methanol 40%) were mixed. The reaction mixture solution was placed at room temperature for 42 h. Colour of reaction solution changed to yellow, then, brown; finally, a brown powder was precipitated. The precipitate was filtered off, washed with distilled water, and alcohol consequently, and then, dried at 105°C for 48 hours.

3. RESULTS AND DISCUSSION

3.1 FTIR Analysis

FTIR spectrum of polypyrrole was recorded in KBr solid disk. Positions of characteristic peaks are observed in Fig. 1. Characteristic peaks of polypyrrole are observed at 3484 cm^{-1} due to the N–H vibration of pyrrole ring, at 3020 and 2973 cm^{-1} due to in-plane vibration of aromatic C–H. Bands at 1112, 912, 780, and 657 cm^{-1} are due to out-of-plane vibrations of C–H. C=C and C–C stretchings of the pyrrole rings are observed at 1578, 1485 and 1105 cm^{-1} . C=N and C–N stretchings of pyrrole rings (caused by electron resonance

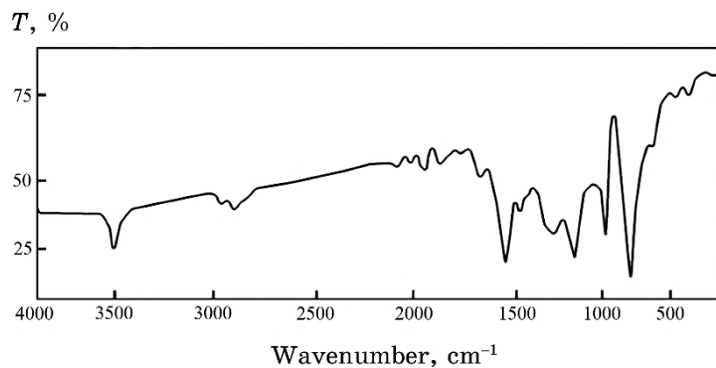


Fig. 1. FTIR spectrum of polyselenophen (KBr disk).

TABLE 1. Comparison of peak positions of the differently synthesized polypyrroles in this work and references.

Bond	This work	References						
		[21]	[22]	[23]	[24]	[25]	[26]	[27]
C–H aromatic	N–H stretching	3500	3500	3522	—	—	3400	3436
	stretching	2980, 2875	2960	—	—	2950	3100	—
	vibrations in plane	918	900	920	902	—	960	1110
	vibrations out of plane	780, 657		811		811	720	757
	C=C	1578, 1485	1475, 1310	1558, 1487	1444	1600	1529	1551, 1554
	C–C	1100	1050	—	—	—	1445	—
pyrrole rings	C–N	1270	1230	1315	1285	1360	1242	—
	C=N	1620	1590	1685	—	1690	1295	—
								1856

and tautomerism in ring) are observed at 1620 and 1270 cm^{-1} . Table 1 shows comparison of peak positions of different polypyrroles synthesized in this work and in references. The spectrum differs slightly from that of the reference polyselenophen due to effects of preparation method.

3.2. XPS Analysis

X-ray photoelectron spectroscopy (XPS) is an excellent technique for analysing the top of 5–10 nm of polymer surface. Figure 2, *a* shows the x-ray photoelectron spectroscopy of PPy polymer. XPS

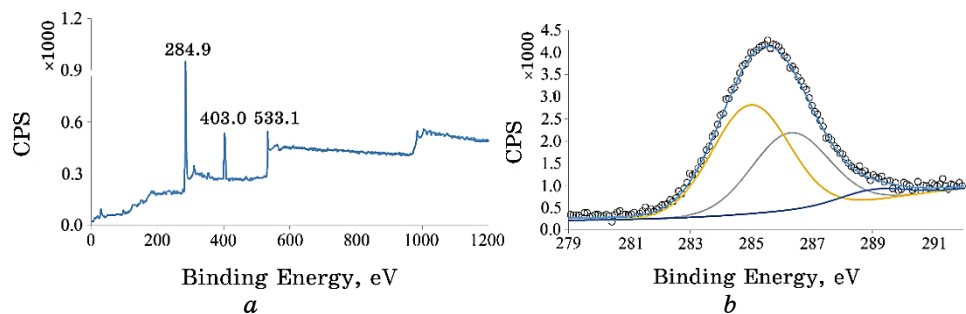


Fig. 2. *a)* XPS spectra for (PPy); *b)* (C1s) spectra with typical peaks.

spectra contain three peaks at 533.1, 403.0 and 284.3 eV due to O1s, N1s and C1s, respectively. This shows polymers' carbon, oxygen and nitrogen. Figure 2, *b* shows analysis of C1s peak. Carbon atoms in polymer are of three kinds: C=C–H (285.1) 50.6%, C–N (286.3) 43.9%, and C=O (289.0) 5.5%; results comply with polymer structure and references [28, 29, 30].

3.3. EDX Analysis

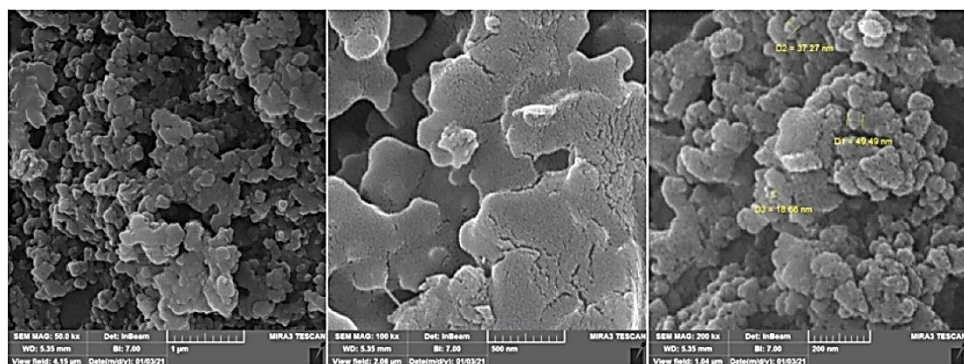
EDX technique measures x-rays emitted from the sample that is subjected to a current of electrons to characterize elemental composition. A current of electrons is scanned across the sample surface inducing emission of x-ray fluorescence from the elements' atoms. Energies of the x-rays are characteristic of the element from which they are emitted [31]. Table 2 shows EDS results for three areas of polymer surface. There is a slight difference in results because EDS analysis is less accurate in determining the ratio of elements. Polymer contains carbon 76.6%, nitrogen 19.1%, and oxygen 1.9%. Ratio N/C is of about 25% (one nitrogen atom for four carbon atoms). Presence of oxygen may be due to the oxidation of some pyrrole rings in the polymer [29].

3.4. SEM

Morphology and surface of polypyrrole particles were studied by scanning electron microscopy (SEM). Figure 3 shows SEM image of polypyrrole. Polymer consists of spherical nanoparticles with average size of about 28 nm and clump together in clusters with rough surface. When checking SEM image of the polymer, a method for forming polymer nanoparticles can be suggested, in which polymer particles grow up to be spherical particles (about 38 nm) and

TABLE 2. EDX analysis for three areas of polymer surface.

Area 3		Area 2		Area 1		Element
atomic, %	wt.%	atomic, %	wt.%	atomic, %	wt.%	
76.60	69.44	77.6	72.6	75.4	66.1	C
19.10	20.20	19.2	20.9	18.6	19.0	N
0.25	0.29	0.25	0.29	0.25	0.29	N/C
1.90	2.29	2.1	2.6	2.3	2.7	O
2.40	7.77	1.1	3.6	3.7	11.9	other
100.25	100.00	100.2	100	100.2	100	total

**Fig. 3.** Photo of polypyrrole polymer under scanning electron microscope (SEM).

merged together forming huge cluster.

3.5. X-Ray Diffraction (XRD)

Crystalline structure of PPy was studied by x-ray diffraction. XRD data were used to determine crystallinity percentage and crystal size. Figure 4, *a* shows the XRD pattern of polymer. XRD spectra were analysed to determine areas of amorphous structure and crystalline structure as well [32]. Crystallinity percentage $P_{cry}\%$ was calculated by Eq. (1) [32, 33]:

$$P_{cry}\% = \frac{A_{cry}}{A_{cry} + A_{Amo}} \times 100, \quad (1)$$

where A_{cry} is sum of area under peak of crystallized structure and A_{Amo} is area under peak of amorphous structure [33]. The crystalline

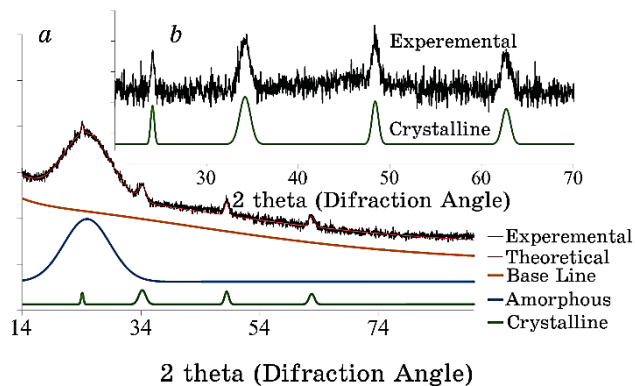


Fig. 4. X-ray diffraction (XRD) for polypyrrole polymer.

TABLE 3. Percentage areas of crystalline peaks and other parameters.

P , %	Crystal Size, nm	Theta, rad	W.H.T., rad $\cdot 10^{-2}$	Peak
7.64%	3.20%	9.42	0.298	P1
	0.86%	30.56	0.210	P2
	1.72%	17.39	0.422	P3
	1.86%	15.54	0.547	P4
92.36%				amorphous

percentage $P_{cry}\%$ was of about 7.64%. Crystals' size was determined by Scherrer equation from crystalline peaks. Figure 4, *b* shows the XRD pattern of PFPy; peaks at 24.1, 24.2, 48.4 and 62.7° belong to crystalline phase; peak at 24.9° belongs to amorphous phase [34]. Table 3 shows crystal size, percentage of crystalline peaks and other parameters. Average crystal size is of 15.1 nm. Polypyrrole is semi-crystalline with particles consisting of an amorphous shell and crystalline core. Crystallization ratio corresponds to the core/shell weight ratio. Using the data in Table 3, we have calculated the true size of particles using Eq. (2) [35]:

$$D_r = \sqrt[3]{\frac{D^3}{P_{cry}\%}} \times 100 , \quad (2)$$

where D_r particle size, and D is crystal size. Calculated average particle size is of 35.59 nm, while it is of about 38 nm. Particle size by XRD is more accurate and closer to reality because of large number of particles in sample, and it is not subject to the experience of the analysis as SEM.

4. CONCLUSIONS

Polypyrrole was synthesized using ammonium persulfate as oxidizing agent in methanol 40%. Structure of polypyrrole was characterized by FTIR, XPS and EDX. Polymer particles are spherical (with size of about 38 nm by SEM) clumping together and forming clusters. Polypyrrole morphology is semi-crystalline; particles consist of an amorphous shell fraction and crystalline core with size of 15.1 nm. Particle size by XRD data was of 35.59 nm.

5. HIGHLIGHTS

Nanoparticles of polypyrrole have been synthesized and characterized by a simple and easy method.

Morphology of resulting polymer was studied by SEM.

Crystalline structure and particle size of polypyrrole was studied by XRD (size was of about 35.59 nm).

Particles size was determined by SEM and compared with XRD.

ACKNOWLEDGEMENT

The authors feel great thanks and gratitude to Prof. Hassan Kalawi and Ms. Marwa Al-Keder.

REFERENCES

1. A. K. Mishra, *Condensate & Nano Physics*, **5**, No. 2: 159 (2018);
[doi:10.26713/jamcn.v5i2.842](https://doi.org/10.26713/jamcn.v5i2.842)
2. J. C. Scott, *Nanostructured Conductive Polymers*, **1**, No. 1: 1 (2010);
[doi:10.1002/9780470661338.ch1](https://doi.org/10.1002/9780470661338.ch1)
3. N. Yi and M. R. Abidian, *Biosynthetic Polymers for Medical Applications*, **1**, No. 4: 243 (2016); [doi:10.1016/b978-1-78242-105-4.00010-9](https://doi.org/10.1016/b978-1-78242-105-4.00010-9)
4. B. X. Valderrama-García, E. Rodríguez-Alba, E. G. Morales-Espinoza, K. M. Chane-Ching and E. Rivera, *Molecules*, **21**, No. 172: 1 (2016);
[doi:10.3390/molecules21020172](https://doi.org/10.3390/molecules21020172)
5. R. Li, Y. Mo, R. Shi, P. Li, C. Li, Z. Wang, and S. Li, *Monatshefte für Chemie — Chemical Monthly*, **145**, No. 1: 85 (2013); [doi:10.1007/s00706-013-1051-2](https://doi.org/10.1007/s00706-013-1051-2)
6. T. Yamamoto, T. Maruyama, Z.-H. Zhou, T. Ito, T. Fukuda, Y. Yoneda, and S. Sasaki, *Journal of the American Chemical Society*, **116**, No. 11: 4832 (1994); [doi:10.1021/ja00090a031](https://doi.org/10.1021/ja00090a031)
7. R. Kumar, S. Singh, and B. C. Yadav, *Engineering and Technology*, **2**, No. 11: 110 (2015); [doi:10.17148/IARJSET.2015.21123](https://doi.org/10.17148/IARJSET.2015.21123)
8. R. Ansari, *E-Journal of Chemistry*, **3**, No. 4: 186 (2006).
9. N. V. Blinova, J. Stejskal, M. Trchová, J. Prokeš, and M. Omastová, *European Polymer Journal*, **43**, No. 2331: (2007);

- [doi:10.1016/j.eurpolymj.2007.03.045](#)
10. W.-L. Yuan, X. Yang, L. He, Y. Xue, S. Qin, and G.-H. Tao, *Frontiers in Chemistry*, **6**: 1 (2018); [doi:10.3389/fchem.2018.00059](#)
11. T. V. Vernitskaya and O. N. Efimov, *Russian Chemical Reviews*, **66**, No. 5: 443 (1997); [doi:10.1070/rc1997v066n05abeh000261](#)
12. A. J. Epstein, *Springer Science Business Media*, **1**, No. 1: 725 (2007).
13. L. Cabrera, S. Gutierrez, M. P. Morales, N. Menendez, and P. Herrasti, *Journal of Magnetism and Magnetic Materials*, **321**, No. 14: 2115 (2009); [doi:10.1016/j.jmmm.2009.01.021](#)
14. B. R. Scharifker, E. García-Pastoriza, and W. Marino, *Journal of Electroanalytical Chemistry and Interfacial Electrochemistry*, **300**, Nos. 1–2: 85 (1991); [doi:10.1016/0022-0728\(91\)85385-3](#)
15. L. Cabrera, S. Gutierrez, M. Morales, N. Menendez, and P. Herrasti, *Journal of Magnetism and Magnetic Materials*, **321**, No. 14: 2115 (2009); [doi:10.1016/j.jmmm.2009.01.021](#)
16. G. Vázquez-Rodríguez, L. Torres-Rodríguez, and A. Montes-Rojas, *Desalination*, **416**, No. 1: 94 (2017); [doi:10.1016/j.desal.2017.04.028](#)
17. S. Asavapiriyanon, G. Chandler, G. A. Gunawardena, and D. Pletcher, *Journal of Electroanalytical Chemistry and Interfacial Electrochemistry*, **177**, Nos. 1–2: 229 (1984); [doi:10.1016/0022-0728\(84\)80225-9](#)
18. Y. Shao, J. Wang, H. Wu, J. Liu, I. A. Aksay, and Y. Lin, *Electroanalysis*, **22**, No. 10: 1027 (2010); [doi:10.1002/elan.200900571](#)
19. D. Reynaerts, J. Peirs, and H. Van Brussel, *Physical*, **61**, Nos. 1–3: 455 (1997); [doi:10.1016/s0924-4247\(97\)80305-6](#)
20. T.-M. Wu, H.-L. Chang, and Y.-W. Lin, *Composites Science and Technology*, **69**, No. 5: 639 (2008); [doi:10.1016/j.compscitech.2008.12.010](#)
21. M. T. Ramesan and V. Santhi, *Composite Interfaces*, **25**, No. 8: 725 (2010). [doi:10.1080/09276440.2018.1439626](#)
22. M. A. Chougule, S. G. Pawar, P. R. Godse, R. N. Mulik, S. Sen, and V. B. Patil, *Soft Nanoscience Letters*, **01**, No. 1: 6 (2011); [doi:10.4236/sn.2011.11002](#)
23. T. A. Nascimento, F. V. Avelar Dutra, B. C. Pires, C. R. Teixeira Tarley, V. Mano, and K. B. Borges, *RSC Advances*, **6**, No. 69: 64450 (2016); [doi:10.1039/c6ra14071h](#)
24. K. Arora, A. Chaubey, R. Singhal, R. P. Singh, M. K. Pandey, S. B. Samanta, and S. Chand, *Biosensors and Bioelectronics*, **21**, No. 9: 1777 (2006); [doi:10.1016/j.bios.2005.09.002](#)
25. B. Tian and G. Zerbi, *The Journal of Chemical Physics*, **92**, No. 6: 3886 (1990); [doi:10.1063/1.457794](#)
26. H. J. Kharat, K. P. Kakde, P. A. Savale, K. Datta, P. Ghosh, and M. D. Shirsat, *Polymers for Advanced Technologies*, **18**, No. 5: 397 (2007); [doi:10.1002/pat.903](#)
27. H. N. Muhammad Ekramul Mahmud, A. K. O. Huq, and R. Yahya, *RSC Advances*, **6**, No. 18: 14778 (2016); [doi:10.1039/c5ra24358k](#)
28. I. Losito, C. Malatesta, L. Sabbatini, and P. G. Zambonin, *Surface Science Spectra*, **3**, No. 4: 375 (1994); [doi:10.1116/1.1247790](#)
29. C. Chan and L.-T. Weng, *Materials*, **9**, No. 8: 655 (2016); [doi:10.3390/ma9080655](#)
30. M. Šetka, R. Calavia, L. Vojkůvká, E. Llobet, J. Drbohlavová, and S. Vallejos, *Scientific Reports*, **9**, No. 1: 1 (2019); [doi:10.1038/s41598-019-](#)

44900-1

31. J. Bergström, *Experimental Characterization Techniques. Mechanics of Solid Polymers* (Elsevier: 2015), p. 19–114 (2015); doi:[10.1016/B978-0-323-31150-2.00002-9](https://doi.org/10.1016/B978-0-323-31150-2.00002-9)
32. A. S. Marf, R. M. Abdullah, and S. B. Aziz, *Membranes*, **10**, No. 4: 71 (2020); doi:[10.3390/membranes10040071](https://doi.org/10.3390/membranes10040071)
33. B. Aziz, S. Marf, A. Dannoun, E. M. Brza, and R. M. Abdullah, *Polymers*, **12**, No. 10: 2184 (2020); doi:[10.3390/polym12102184](https://doi.org/10.3390/polym12102184)
34. Ch. He, Ch. Yang and Yo. Li, *Synthetic Metals*, **139**, No. 2: 539 (2003); doi:[10.1016/s0379-6779\(03\)00360-6](https://doi.org/10.1016/s0379-6779(03)00360-6)
35. A. Al-Hamdan, A. Al-Falah, F. Al-Deri, and I. Al-Ghoraibi, *Nanosistemi, Nanomateriali, Nanotehnologii*, **20**, Iss. 1: 195 (2022); https://www.imp.kiev.ua/nanosys/media/pdf/2022/1/nano_vol20_iss1_p0195p0205_2022.pdf